Ann. Geophys., 29, 1305–1315, 2011
www.ann-geophys.net/29/1305/2011/
doi:10.5194/angeo-29-1305-2011

Annales Geophysicae

IMF B_y effects in the plasma flow at the polar cap boundary

R. Lukianova[1,2] **and A. Kozlovsky**[3]

[1]Arctic and Antarctic Research Institute, St. Petersburg, Bering Str. 38, 199397, Russia
[2]Space Research Institute, Moscow, Profsoyuznaya Str. 84/32, 199397, Russia
[3]Sodankylä Geophysical Observatory of the University of Oulu, P.O. Box 3000, 90014, Finland

Received: 5 December 2010 – Revised: 14 June 2011 – Accepted: 21 June 2011 – Published: 22 July 2011

Abstract. We used the dataset obtained from the EISCAT Svalbard Radar during 2000–2008 to study statistically the ionospheric convection in a vicinity of the polar cap boundary as related to IMF B_y conditions separately for northward and southward IMF. The effect of IMF B_y is manifested in the intensity and direction of the azimuthal component of ionospheric flow. The most significant effect is observed on the day and night sides whereas on dawn and dusk the effect is essentially less prominent. However, there is an asymmetry with respect to the noon-midnight meridian. On the day side the intensity of B_y-related azimuthal flow is maximal exactly at noon, whereas on the night side the maximum is shifted toward the post-midnight hours (∼03:00 MLT). On the dusk side the relative reduction of the azimuthal flow is much larger than that on the dawn side. Overall, the magnetospheric response to IMF B_y seems to be stronger in the 00:00–12:00 MLT sector compared to the 12:00–24:00 MLTs. Quantitative characteristics of the IMF B_y effect are presented and partly explained by the magnetospheric electric fields generated due to the solar wind and also by the position of open-closed boundary for different IMF orientation.

Keywords. Ionosphere (Plasma convection)

1 Introduction

The structure of high-latitude ionospheric plasma convection is controlled by the IMF and depends primarily on the IMF strength and orientation in the GSM Y-Z plane (Heppner and Maynard, 1987). If IMF B_z is directed southward or equal to zero, the ionospheric projection of the magnetospheric plasma circulation is a two-cell convection pattern with a fairly homogenous central anti-sunward flow. The viscous processes at the magnetospheric boundary form the similar, though less intensive, convection pattern. If B_z is directed northward and strong enough, additional flow cells with a sunward cross-polar cap flow are developed.

The IMF B_y modifies the twin-cell convection patterns and leads to the dawn-dusk asymmetry which is, in general, antisymmetric in the opposite hemispheres. In a given hemisphere the effect is quasi-mirrored with respect to the noon meridian for opposite signs of B_y. Basic physical ideas of the IMF B_y effects on magnetospheric electrodynamics were suggested more than 30 yr ago (Nishida, 1971; Jørgensen et al., 1972; Stern, 1973; Leontyev and Lyatsky, 1974). In previous studies the IMF B_y-related dawn-dusk asymmetry in polar cap convection and the associated Svalgaard-Mansurov effect (Svalgaard, 1973) have been widely attributed to the magnetic tension forces acting on open field lines. The paradigm is as follows (Jørgensen et al., 1972; Khan and Cowley, 2001). The flows are believed to be due the effect of the magnetic tension force acting on the newly reconnected flux tubes in the presence of IMF B_y. For $B_y > 0$, open tubes are pulled westward in the Northern Hemisphere and added to the dawn side of the northern tail lobe, while simultaneously being pulled eastward in the Southern Hemisphere and added to the dusk side of the southern tail lobe and vice versa for $B_y < 0$. Thus, the anti-sunward flow over the polar cap is asymmetric with stronger flows on the dawn side in the Northern Hemisphere and on the dusk side in the Southern Hemisphere for $B_y > 0$, and vice versa for $B_y < 0$. The overall effect on open field lines is an additional westward (eastward) circulation in the Northern Hemisphere if $B_y > 0$ ($B_y < 0$), and vice versa in the Southern Hemisphere.

Correspondence to: R. Lukianova
(renata@aari.nw.ru)

Published by Copernicus Publications on behalf of the European Geosciences Union.

The B_y-related effect may be also interpreted in such a way that the convection asymmetry is formed by two elements (Nishida, 1971; Leontyev and Lyatsky, 1974; Kozlovsky et al., 2003). Firstly, the IMF B_y component irrespective of its sign causes anti-sunward transpolar flow due to reconnection at the flanks of the magnetosphere. In the Northern Hemisphere this flow is stronger on the dawn (dusk) side. It adds a westward (eastward) circulation when IMF B_y is positive (negative). Secondly, the IMF B_y generates a voltage between the two magnetospheric lobes. The IMF is frozen in the solar wind plasma that moves away from the Sun with a typical speed of $\sim$300 km s^{-1}. As a result, the IMF generates an electric field $\boldsymbol{E}_{\rm sw} = -\boldsymbol{V}_{\rm sw} \times \boldsymbol{B}_{\rm IMF}$ in the Earth-fixed framework. In particular, the IMF B_y (positive direction from dawn to dusk) generates an electric field directed from South to North. From the voltage between the two polar caps, one can expect a radial electric field and, consequently, an azimuthal (around the pole) plasma flow, which is opposite in the northern and Southern Hemispheres. For instance, a negative IMF B_y produces an eastward (westward) plasma flow within the northern (southern) polar cap.

In a steady-state case, such oppositely directed flows should not co-exist in the closed magnetic field line regions of the conjugate hemispheres because of high conductivity along the magnetic field lines. Hence it was commonly believed that the asymmetric plasma flows occur within the open polar caps forming lobe convection cells. However, recent observations have shown that the anti-symmetric electric field penetrates to the region of closed magnetic field lines. This phenomenon may be explained by the anomalous resistance associated with the inter-hemispheric field-aligned currents (Kozlovsky et al., 2003). Sandholt and Farrugia (2009) showed that the situation may be even more complicated. Namely, plasma convection on open field lines can be subdivided in two distinct stages corresponding to "newly open" and "old open" (reconnection has occurred some time earlier) field lines. Convection channels in the second stage play an important role in the excitation of an IMF B_y-related dawn-dusk convection asymmetry. These flow channels indicate momentum transfer from the solar wind along the "old open" field lines associated with polar rain precipitation. In addition, the inter-hemispheric asymmetry may be due to the specific mapping of the reconnection electric field to the ionosphere. This was shown by Watanabe at al. (2007), who studied a topological model of the IMF-magnetosphere reconnection in many details.

Qualitatively, the basic effects of IMF B_y on the high-latitude ionospheric convection have been understood by now. However, we need quantitative characteristics which are important for better understanding of the high-latitude magnetosphere-ionosphere coupling and for calibrating models of ionospheric electrodynamics. An interesting study on the plasma flow related to the IMF B_y was performed by Khan and Cowley (2001), who analyzed a database of 300 h of tristatic ionospheric velocity measurements obtained overhead at Tromsø (66.3° magnetic latitude) by the EISCAT UHF radar system. The authors found that significant flow variations with IMF B_y occur predominantly in the midnight sector (21:00–03:00 MLT) and also in the pre-dusk (16:00–17:00 MLT) sector. The flows are directed eastward for IMF B_y positive and westward for IMF B_y negative, and with magnitudes of the order of 20–30 m s^{-1} nT^{-1} in the midnight sector and 10–20 m s^{-1} nT^{-1} in the pre-dusk sector. At other local times the IMF B_y-related perturbation flows are much smaller, less than 5 m s^{-1} nT^{-1}. These observations relate to the region of closed magnetic field lines.

In the present paper we study the B_y effect at essentially higher latitudes, in a vicinity of the polar cap boundary. We utilize a large (more than 1300 h) database collected during 8 yr at the EISCAT Svalbard Radar (around 75° MLat). Our aim is to infer quantitative characteristics of the east-west ionospheric plasma flow associated with IMF B_y. After description of the collected data (Sects. 2 and 3) we present the statistical results of the dependence of the flow speed on IMF B_y in different MLT sectors (Sect. 4). In Sect. 5 we show the dawn/dusk asymmetry feature in association with the IMF B_y. Discussion is given in Sect. 6. The final section is a summary of the obtained results.

2 Data and method

The EISCAT Svalbard Radar (ESR) has a unique location that is convenient for monitoring the ionospheric plasma parameters in a vicinity of the polar cap boundary. For the present study the data were obtained from the Common Program 2 (CP2) ESR measurements. During 2000–2008, the radar was working more than 1300 h in the CP2 mode with the beam being periodically alternated between three positions (one vertical and two elevated at 63° or 66° to horizon with azimuth angles 172° and 144°, respectively). Under an assumption that the plasma flow is spatially uniform over the region of ESR observations and does not change during the scanning cycle, vector of the large-scale plasma flow in the F-region was calculated and the electric field vector was inferred, assuming that the F-region plasma experience the $\boldsymbol{E} \times \boldsymbol{B}$ drift. These measurements refer to the heights of 200–300 km with spatial resolution of the order of 100 km in the horizontal plane. These data are related to about 74.5° MLat. The scanning cycle was typically about 6 min. We used all triads of consequent antenna positions to calculate the vector flow. In this case each a measurement contributes to three data points. Thus, although the sampling rate of the ESR data is about 2 min, the data was averaged over the interval of about 6 min.

The ESR data are uniformly distributed along local time. The majority of the data (57 %) were obtained near the autumn equinox (September and October). For summer conditions (June–July) there existed 24 % of the data, while 16 % of the data were obtained during February–March (spring),

and only 3 % of the data were obtained during winter (December).

For the present study we have calculated the azimuthal eastward component of plasma flow, V_E, (i.e. along L-shell), which is at 20 deg. from geographic East to North. The plasma flow data were combined with the data on IMF Y- and Z-components (GSM) obtained from the OMNI database. The OMNI provides interplanetary parameters referred to the Earth's orbit (1 AU). We utilised the data averaged over 5-min interval, which match to the radar data. The analysis is made separately for the northward IMF ($B_z > 0$) and the southward IMF ($B_z < 0$).

The main parameters studied are correlation and linear regression of V_E with IMF B_y. The correlation coefficient C_{corr} calculated in the conventional way, and confidence intervals for the correlation coefficients are calculated using the following formula:

$$\delta C_{corr} = t_\gamma \frac{1 - C_{corr}^2}{\sqrt{n}}, \quad (1)$$

where n is the number of data points and t_γ is the inverse standardized normal distribution (for the 95 % confidence interval, $t_\gamma = 1.96$). The linear regression coefficient K is calculated by the least square method to get a linear approximation

$$V_E = V_{E0} + K B_Y. \quad (2)$$

where V_{E0} is a background part of azimuthal flow that does not depend on a sign of IMF B_y. This flow basically relates to the two-cell convection pattern generated by the reconnection and viscous interaction on the magnetopause.

Note that in the Northern Hemisphere, a duskward (i.e. positive) IMF B_y generates a westward (i.e. negative) plasma flow and, vice versa, a negative IMF B_y generates an eastward (i.e. positive) flow around the polar cap. Hence, the coefficient K is normally negative. Because of that we use reverse axis direction for plotting K below. Strictly speaking, the correlation coefficients are also negative, however, we use below the absolute value of the coefficients to characterize just a degree of linear dependence.

3 Response time of ionospheric convection to IMF B_y

The first our step is to determine the time lag between the IMF B_y conditions at 1 AU and the corresponding ionospheric plasma flow at the ESR location. The ionospheric convection response to a change in the IMF as measured by the spacecraft is a sum of the following time intervals: (1) the propagation time for the IMF to reach the at the front side magnetopause (assumed to be typically located at X GSE = 10 Re), (2) the magnetosphere-ionosphere communication time, and (3) the ionospheric convection reconfiguration time (Zhang et al., 2007).

In the present study the time interval (1) is neglected because we use the OMNI data which provides interplanetary parameters referred to the Earth's orbit. Thus we need to estimate the sum of intervals (2) and (3). There are two possible approaches to determine the convection response to a change in the IMF. The first is to examine each individual event of the IMF change to perform a search of the associated details of the response. Such an analysis is more appropriate for the study of the response to a sudden change in the IMF orientation (e.g. Hairston and Heelis, 1995; Ridley et al., 1998; Kabin et al., 2003; Lyons et al., 2003). The second approach is to average the data for revelation the most common features. Such approach is used for construction of the statistical models with binning of both IMF and ionospheric data (e.g. Heppner and Maynard, 1987; Papitashvili and Rich, 2002; Zhang et al., 2007). In the frame of this approach the slow variations of the IMF may be accounted for.

In order to determine the lag time which provides the largest acceleration of the azimuthal flow in response to a strengthening of the IMF B_y, we compared the measured V_E values with time series of the IMF B_y. We considered various lags between the two data sets, from −100 to 300 min through 5 min. For each lag time, correlation (C_{corr}) and regression (K) coefficients between V_E and IMF B_y were calculated, separately for southward and northward IMF. Due to the Earth rotation, the radar data come from different MLT. With no separation on MLT, both the correlation and regression coefficients show maxima at lag times 35 min and 15 min under the south- and northward IMF conditions, respectively. However, the convection on day side may respond faster than that one on the night side (Lockwood et al., 1989). As one might expect different lag times for the day and night sides, we also calculate the coefficients separately for the 06:00–18:00 and 18:00–06:00 MLT sectors. In Fig. 1 the regression coefficient versus the lag time is presented. The left and right panel represents the southward and northward IMF conditions, respectively, whereas the top and bottom panel corresponds to the day and night side, respectively. Vertical lines indicate the lag times of 35 min (left panels) and 15 min (right panels).

One can see that under the southward IMF conditions the shape of dayside and nightside curves are quite similar with the lag time of about 35 min for both. When the IMF is northward, the situation is less clear and it is rather difficult to distinguish single maxima. The most probable dayside lag time can be determined at ∼15 min. The nightside lag time is rather uncertain within 0–70 min and there is no essential K dependency on the lag time within this interval. The lag time show a tendency to be larger at the night side, however, the maxima are rather flat. Below we assume the 15 min lag time for the northward IMF and 35 min for the southern IMF that is quantitatively consistent with previous estimates.

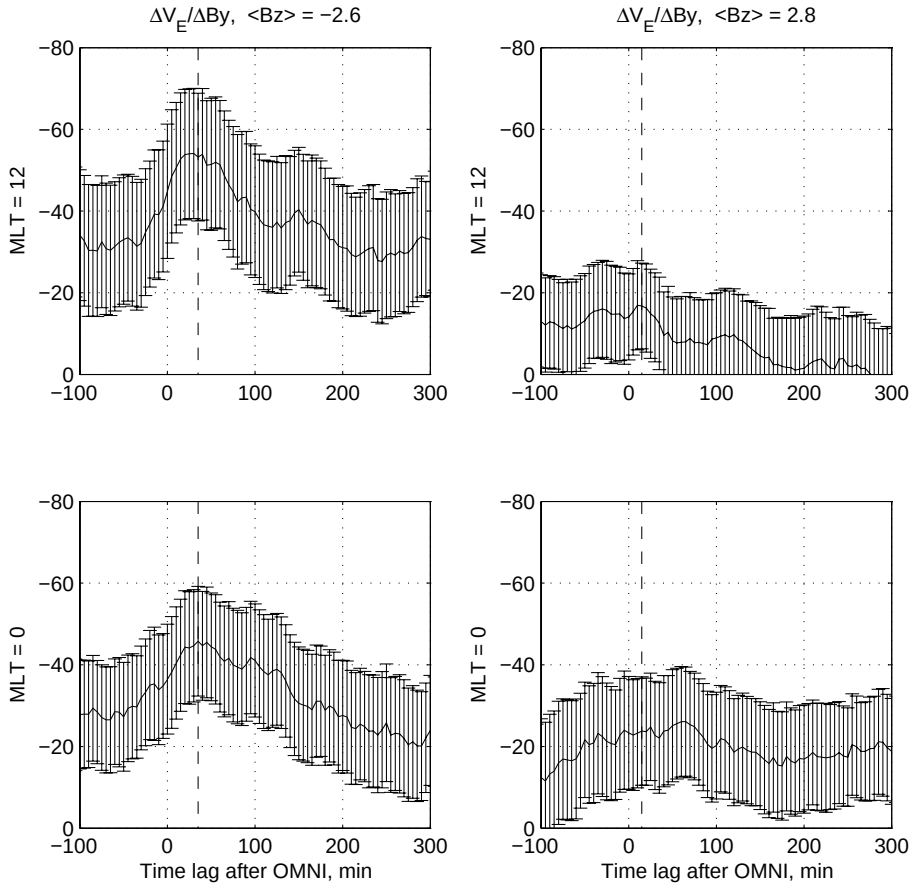

Fig. 1. The regression coefficients against the lag time for southward (left) and northward (right) IMF. Top and bottom panels correspond to the day and night side, respectively. Vertical lines indicate the lag times 35 min and 15 min.

We should emphasize that our aim here is to determine only the lag time that should be accounted for comparison the ionospheric data at ESR location with the OMNI data. These lags do not necessarily correspond to the rearrangement of the entire convection pattern in response to the IMF B_y changes since at a given UT interval the radar is able to measure the response at the particular location but not an overall change in large-scale convection. However, the above consideration suggests that the B_y-related flow averaged along the latitudinal circle near the polar cap boundary may be considered as established (relative to OMNI data) after a suitable lag time of 35 min and 15 min for IMF $B_z < 0$ and $B_z > 0$, respectively.

4 IMF B_y control of the azimuthal plasma flow in different MLT sectors

The ESR measurements cover the entire MLT range with a fairly uniform local time distribution. We separated the whole set of velocity data into 3 h wide sectors centred at 00:00, 03:00, 06:00, 09:00, 12:00, 15:00, 18:00 and 21:00 MLTs. Figure 2 presents the dependence of the azimuthal plasma flow V_E upon the IMF B_y, when the IMF B_z is southward. Each plot represents the corresponding MLT sector and the plots are organized according to the normal MLT circle so that the flows at different locations can be easily compared. Each dot in the plot represents the average over 100 actual data points. To obtain them, the data were sorted according to IMF B_y in ascending order in a given MLT sector. After that an averaged value of V_E and B_y for each 100-point data sequence was calculated. Distributions of the dots demonstrate clearly a linear dependence of V_E upon IMF B_y. Namely, the eastward (westward) V_E increases with the increase of negative (positive) B_y. Straight line in each plot shows the linear approximation. It is easy to see, however, that the slope of the fit line (represented by K), its position about the axis and the scattering of points (represented by C_{corr}) are not the same at different MLT. In the dawn side the slope is steep, implying a stronger response of V_E to the B_y change. In the dusk side the slope is smaller. In the 12:00, 15:00 and 18:00 MLT sectors V_E values are mostly negative, which indicate the predominantly westward flow that is likely a part of low-latitude return flow. In the noon

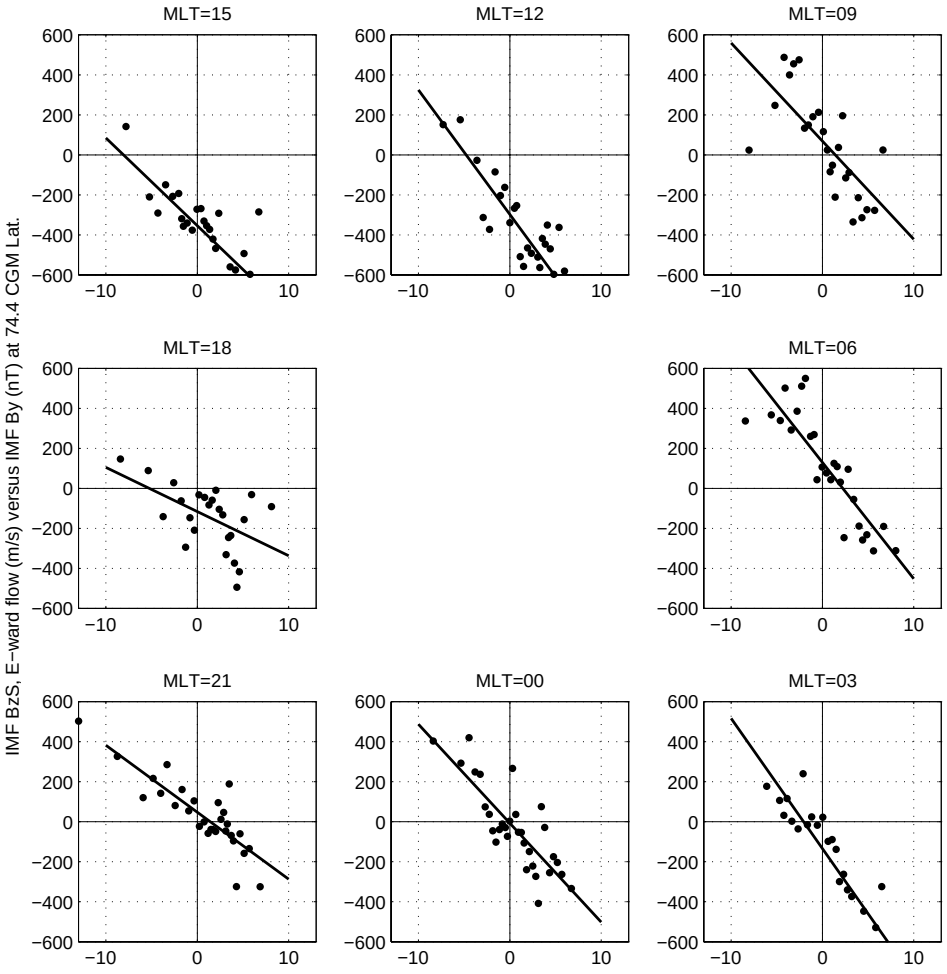

Fig. 2. Dependence of the eastward plasma flow (V_E) on the IMF B_y in the eight 3-h MLT sectors for the IMF $B_z < 0$.

sector there are only two data points with positive (eastward) flow. This depicts the overall prevalence of the dusk cell that adds more westward flow near the polar cap boundary.

The prevalence of the westward flow at noon may be associated with the inherent asymmetry of the two-cell convection pattern observed even for $B_y = 0$. The cells are not exactly symmetric, with a larger cell and a higher potential on the dusk side. The effect was schematically described first by Atkinson and Hutchison (1978). These authors pointed out that the day-night conductivity gradient in the polar cap E-region ionosphere squeezes the antisunward convective flow to the dawnside of the polar cap. This is a likely cause of the lack of the mirror symmetry in the flow pattern that, as theory indicates, should exist in away and toward solar sectors in the Northern Hemisphere in summer. The day-night conductivity gradient in the E-region ionosphere causes such an effect due to the Hall current closure of the Region 1 field-aligned current. Ruohoniemi and Greenwald (2005) mentioned the fact that the statistical convection pattern for $B_y < 0$ is most asymmetrical during winter, whereas that for positive $B_y > 0$ is most asymmetrical during summer. Note that the majority of the ESR data are from summer/equinox. Sandholt and Farrugia (2007) presented the case studies of the dynamical evolution of dayside poleward moving auroral forms (PMAFs) in relation to plasma convection during intervals of southeast and southwest IMF orientations when $|B_y/B_z| > 1$. The observations were made during winter season in Ny Alesund, Svalbard at 76° MLAT, i.e. almost at the same site as the ESR measurements. It was shown that PMAF activity is closely associated with vortical flows in the dawn- and dusk-centered convection with clear B_y-related dawn-dusk asymmetries. However, the large-scale convection does not show the identically mirrored response to the opposite signs of B_y.

Thus a prevalence of the westward flow in Fig. 2 may be caused by the larger widening of the dusk convection cell in comparison with the dawn cell especially at the sunlit ionosphere.

Similar analysis was made for the northward IMF conditions. The results are presented in Fig. 3 which is organized in the same way as the Fig. 2. Even visual inspection of the plots reveals a weaker (relative to the $B_z < 0$ case) relationship between V_E and B_y, especially in the dusk-postnoon

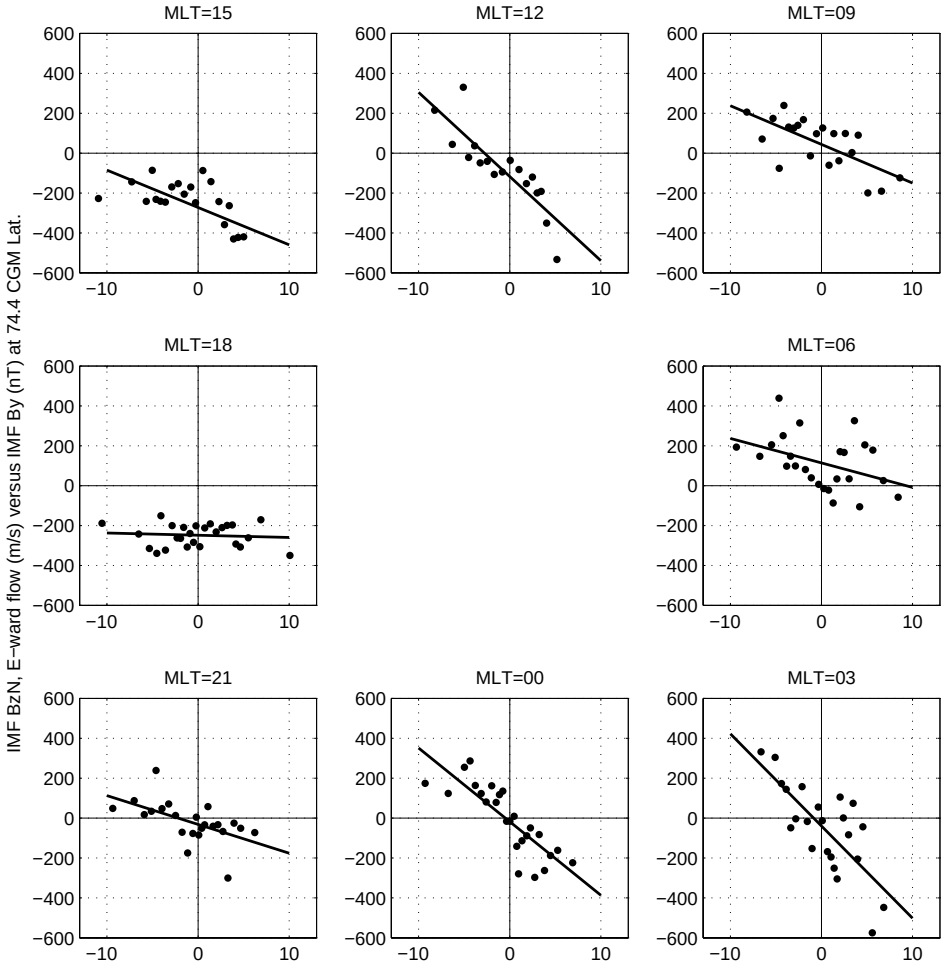

Fig. 3. Same as Fig. 2, but for $B_z > 0$.

sector, where V_E is westward irrespective of a B_y sign, and near dawn where V_E is primarily eastward. Such flow is likely a manifestation of the two-cell convection pattern with sunward (anti-sunward) flow on dusk (dawn). More tight dependence between V_E and IMF B_y is seen at the noon-prenoon and midnight-premidnight hours.

The values of regression coefficient K and correlation coefficient C_{corr} for the linear approximation of V_E and IMF B_y relationship are given in Table. The first column in the table indicates the central hour of 3-h MLT intervals where the data were collected. The second column presents the intensity of the background azimuthal flow V_{E0}. The third and the fourth column presents the regression and correlation coefficient, respectively. The fifth column indicates the total duration of the observations for each MLT sector. Totally, there were 1343 h of observations. Among them, 725 h were during periods of IMF $B_z < 0$, and 618 h were during periods of IMF $B_z > 0$. Mean IMF B_z value for the two subsets of data was -2.6 and $+2.8$ nT, respectively.

Figure 4 summarises the information presented in Figs. 2 and 3 and shows the quantitative characteristics of the sensitivity of the azimuthal flow to the change of IMF B_y at different MLTs. The values of C_{corr} (upper panel) and K (middle panel) in different MLT sectors, separately for IMF $B_z < 0$ and $B_z > 0$, are presented. The lower panel of Fig. 4 shows the position of the polar cap boundary which will be discussed in Sect. 5. For all parameters the eight points actually obtained for the corresponding MLT sectors are connected by the smooth curve using the Fourier interpolation.

From the two upper plots of Fig. 4 one can see the following. Both the regression and correlation coefficients show similar behaviour under the northward and southward IMF conditions, although the B_y-related azimuthal flow is stronger when $B_z < 0$. The MLT profile of K indicates that the IMF B_y effect is maximal near noon and post-midnight ($\sim$03:00 MLT) where its magnitude is about 60 m s^{-1} nT^{-1} for $B_z < 0$. If $B_z > 0$, K is about 40 m s^{-1} nT^{-1} for both the day and night sides. The deepest minimum is seen on dusk ($\sim$18:00 MLT) for both signs of IMF B_z. The other

Table 1. The background flow, regression (K) and correlation ($C_{\rm corr}$) coefficients for the linear approximation of the relationship between $V_{\rm E}$ and IMF B_y; total duration of the observations for each MLT sector.

IMF B_z	MLT	$V_{\rm E0}$, m s^{-1}	K, m s^{-1} nT^{-1}	$C_{\rm corr}$	Duration, h
IMF $B_z<0$	0	-8 ± 43	-49 ± 12	0.82 ± 0.11	105
	3	-134 ± 49	-65 ± 13	0.89 ± 0.08	80
	6	129 ± 50	-58 ± 13	0.87 ± 0.09	87
	9	69 ± 66	-49 ± 19	0.71 ± 0.19	85
	12	-297 ± 55	-62 ± 15	0.85 ± 0.11	88
	15	-354 ± 41	-44 ± 11	0.83 ± 0.11	101
	18	-116 ± 54	-22 ± 14	0.53 ± 0.29	81
	21	47 ± 33	-33 ± 7	0.86 ± 0.09	98
IMF $B_z>0$	0	-18 ± 36	-37 ± 10	0.83 ± 0.12	86
	3	-40 ± 56	-46 ± 16	0.75 ± 0.18	78
	6	114 ± 46	-12 ± 11	0.40 ± 0.33	84
	9	44 ± 36	-19 ± 8	0.68 ± 0.23	71
	12	-117 ± 42	-42 ± 11	0.86 ± 0.12	60
	15	-273 ± 42	-19 ± 9	0.63 ± 0.26	72
	18	-249 ± 21	-1 ± 5	0.09 ± 0.38	88
	21	-32 ± 33	-14 ± 8	0.56 ± 0.28	80

minimum seen at the morning hours (06:00–09:00 MLT) is less prominent for $B_z<0$ and essentially more prominent for $B_z>0$. Similarly, $C_{\rm corr}$ exhibits two maxima and two minima. The first maximum is exactly at noon, while the second is slightly shifted towards the early morning hours. A remarkable asymmetry feature for both parameters, K and $C_{\rm corr}$, is that the dawnside minimum is less prominent than the duskside one.

5 Position of the polar cap boundary

The demarcation between the closed field lines at lower latitudes and the first open magnetic field line at higher latitudes defines a boundary enclosing the polar cap (known as the polar cap boundary, PCB). As mentioned in Introduction, the IMF B_y generates the round-pole plasma flow within the region of open geomagnetic field lines in the polar cap and also in some part of closed magnetosphere adjacent the polar cap boundary. The flow is directed eastward (westward), if the IMF B_y is negative (positive). Obviously, the flow intensity should increase with the magnitude of IMF B_y, and that is seen in Figs. 2 and 3.

The IMF B_y also affects both the size and the shape of polar cap (e.g. Park et al., 2006). Also, the auroral oval and the polar cap as a whole are shifted towards dawn (dusk) for $B_y>0$ ($B_y<0$) (Cowley et al., 1991; Trondsen et al., 1999). Hence, if the PCB moves with IMF B_y changing, the location of the ESR appears to change with respect to the PCB. As a result, the radar may leave the polar cap and enter the region of the closed field lines. The PCB motion certainly contributes to the regression/correlation coefficient between $V_{\rm E}$ and B_y. The effect is the most expectable in the dusk and dawn sides, where the corresponding eastward and westward low-latitude return flow is a part of the two-cell convection.

Figure 5 shows, in frame of MLT and MLat, an average PCB estimated from the Tsyganenko and Sitnov (2005) (TS-2005) geomagnetic field model with the GEOPACK-2008 software (http://geo.phys.spbu.ru/~tsyganenko/modeling.html). To obtain the PCB line, the ionospheric footprint of the last closed field line for each MLT hour was calculated first and then the points were smoothed by the Fourier interpolation. The mean IMF conditions during the period of observations, i.e. $B_z=\pm2.7$ nT and $B_y=\pm3.4$ nT are taken as the model input parameters. Left and right panels of Fig. 5 show the PCB for $B_y<0$ and $B_y>0$, respectively. Red and blue line corresponds to $B_z>0$ and $B_z<0$, respectively. In each plot the dashed circle shows the latitude of the ESR location. From this figure one can see that according to the magnetic field model for $B_z=-2.7$ nT, the ESR is preferably located on closed field lines in the dayside region and within the polar cap in the nightside region. For the northward IMF conditions ($B_z=+2.7$ nT) the ESR is mostly located on closed field lines being closer to PCB on dusk (dawn) side for $B_y<0$ ($B_y>0$).

Even visual inspection of Figure 5 reveals (at least for $B_z>0$) that the PCB under the opposite B_y conditions is not exactly mirrored with respect to the noon-midnight meridian. For instance, the comparison of the PCB at MLT = 06:00, for $B_y<0$, and MLT = 18:00, for $B_y>0$, shows the latitudinal displacement of 1–2°. For quantitative estimation of

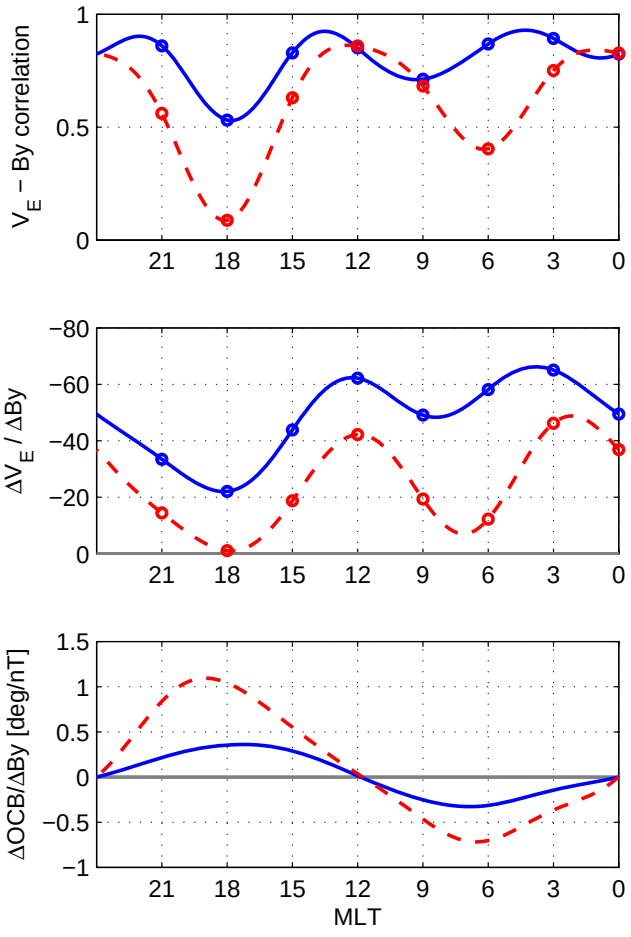

Fig. 4. The values of correlation $C_{\rm corr}$ (upper panel) and regression K (middle panel) coefficients for the $V_{\rm E}$ and IMF B_y relationship for different MLT, separately for IMF $B_z < 0$ and $B_z > 0$. The bottom panel shows the shift of polar cap boundary caused by IMF B_y changes for different MLT. Red and blue curve corresponds to $B_z > 0$ and $B_z < 0$, respectively.

the effect, we calculate the latitudinal shift of PCB per unit of the IMF B_y (nT) at different MLTs. Positive displacement is to the north. The result is presented in Fig. 4, bottom panel. (Here we return to Fig. 4 in order to combine the PCB displacement with $C_{\rm corr}$ and K.) From the bottom panel of Fig. 4 one can see no B_y-related PCB motion at noon and midnight. Hence, the regression coefficient K presented above actually corresponds to the azimuthal flow generated just by the IMF B_y.

The largest PCB shift is seen at about 06:00 and 18:00 MLT. Comparison of the two lower plots in Fig. 4 shows that the largest shift of PCB corresponds to the minima in K. It is not surprising because essential contribution from the low-latitude return flow just on the dusk and dawn sides allows the PCB displacement.

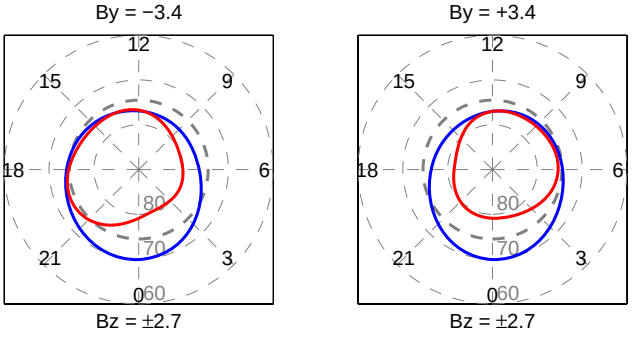

Fig. 5. Position of the polar cap boundary (in the MLT-MLat framework) according to the TS-2005 model for IMF $B_y = -3.4$ nT and $B_y = +3.4$ nT (left and right panel, respectively). Red and blue curve corresponds to $B_z > 0$ and $B_z < 0$, respectively. Dashed circle indicates the position of ESR.

Within the two-cell convection pattern the flow reversal occurs in a vicinity of PCB. In the dusk side the return flow equatorward of PCB is directed to West while the transpolar flow poleward of PCB is directed to East. On the dawn side the directions are opposite. Let us consider the idealized situation when the ESR is situated, for instance, near the dawn meridian. If IMF B_y becomes positive, it results in two effects. Firstly, an additional westward around-pole flow appears within the polar cap. Secondly, the whole polar cap is shifted toward dawn along the 06:00–18:00 MLT meridian. The ESR turns out within the region where the B_y-induced westward flow is superimposed with the eastward transpolar flow. This leads to reduction in $V_{\rm E}$ and decrease of the regression/correlation coefficient in the dusk side. If IMF B_y becomes negative, the polar cap is shifted toward dusk side so that the effect is weak. Similar explanation is valid in the case when the ESR is situated near the dusk meridian. Overall, the IMF B_y-$V_{\rm E}$ dependence is the weakest at 06:00 and 18:00 MLT where the PCB displacement is maximal.

However, it is noteworthy that the duskside PCB displacement is larger than the dawnside one. The difference is more clearly seen, if $B_z > 0$ (Fig. 4, lower panel). Figure 4 shows an additional asymmetry with respect to the noon-midnight meridian that can be hardly explained solely by the dawn-dusk displacement of the PCB. Indeed, an averaged value of the regression coefficient K in the dawn side (00:00–12:00 MLT) exceeds that in the dawn side (12:00–24:00 MLT). For both $B_z < 0$ and $B_z > 0$, the magnitude of K on the dawn side is almost twice larger than that on the dawn side ($\sim$60 vs. $\sim 30\,{\rm m\,s^{-1}\,nT^{-1}}$). Similarly, the correlation between $V_{\rm E}$ and B_y is significantly higher on the dawn side.

6 Discussion

Khan and Cowley (2001) have employed a database of ∼300 h of ionospheric velocity data obtained overhead of Tromso (63.3° MLat) and have analysed them trying to detect the presence of flow effects associated with the IMF B_y. It was found that significant flow variations with IMF B_y occur in the midnight sector and also pre-dusk. The flow velocity and IMF B_y are connected by the proportionality factor of 20–30 (10–20) m s^{-1} nT^{-1} at midnight (pre-dusk). At other local times the IMF B_y-related perturbation flow are much smaller.

We extended the analysis to higher latitudes, where the IMF B_y effect is the most prominent. The ESR (74.5° MLat) measurements provide an opportunity to quantify the dependence of the azimuthal flow speed V_E upon IMF B_y just in the vicinity of the polar cap boundary. The velocity data are obtained from all MLT sectors. The fact that at some time the region of radar measurements is within the polar cap and at the other time it is on the closed field lines provides an additional interesting information on the convection flow, the polar cap displacement and the response of the magnetosphere-ionosphere system to the IMF B_y.

The performed analysis revealed a linear dependence between V_E and IMF B_y at the majority of MLTs. This implies an acceleration of the eastward (westward) flow with an increase of negative (positive) IMF B_y. The average proportionality factor between the two parameters is 48 (24) m s^{-1} nT^{-1} under the southward (northward) IMF conditions. But the fit line has different slopes at different MLTs implying the tightest relationship between V_E and IMF B_y near noon/post-midnight and the weakest one on dusk and dawn.

We found that the main factor modifying the response of V_E is the displacement of the polar cap boundary along the dusk-dawn meridian controlled by the IMF B_y. The PCB displacement can explain the existence of two minima and two maxima in the MLT profile of the V_E and B_y relationship. On the dawn and dusk sides the PCB shift reaches several degrees in latitude, according to TS-05 model. The radar therefore appears in the region where the B_y-related azimuthal flow and the DP2 transpolar flow are oppositely directed, resulting in its mutual suppression. On the other hand, a tight relationship between V_E and IMF B_y is obtained at noon and near midnight, where the TS-05 shows no PCB shift. These observational results support the idea of the B_y-generated interhemispheric voltage, radial electric field and the round-pole plasma flow in the ionosphere (Lyasky, 1978; Kozlovsky et al., 2003).

In addition to the dawn/dusk minimum and noon/midnight maximum in the MLT profile a remarkable asymmetry feature is revealed in the sensitivity of the azimuthal flow to the change of IMF B_y. Particularly, putting a separation line along the noon-midnight meridian and comparing the dusk and dawn sides, one can notice that for a given intensity of IMF B_y the V_E in the 00:00–12:00 MLT sector is generally larger than the corresponding V_E in the 12:00–24:00 MLT sector. Also, the night-time maximum is not exactly at midnight, but shifted towards the post-midnight hours.

The dawn-dusk asymmetry can be associated with the large-scale convection. It is well known that the full convection patterns do not demonstrate a simple mirroring across the noon-midnight meridian if a sign of B_y is changed (Ruohoniemi and Greenwald, 2005; Papitashvili and Rich, 2002; Lukianova and Christiansen, 2006; Lukianova et al., 2008). In the Northern Hemisphere, the duskside vortex of convection pattern expands over the noon meridian even without influence of IMF B_y. The effect is interpreted as a result of the interaction of the initially mirror-symmetric IMF B_y pattern with the ionospheric conductivity distribution or the magnetospheric topology. Large and intense duskside vortex contributes to the B_y-related azimuthal flow just on the dawn side, where the response of V_E to the IMF B_y change is more pronounced. Interestingly, the TS-05 model predicts some dawn-dusk asymmetry of the PCB shift related to IMF B_y. The PCB shift is slightly larger (by about 1° MLat) on the dusk side than on the dawn side, the effect is seen better, if $B_z > 0$.

The IMF B_x component may play a role. Using global MHD simulations Peng et al. (2010) investigated the IMF B_x effect on SW-M-I coupling. Although the analysis was limited to the case of IMF $B_y = 0$ an interesting result has been obtained. In particular, for low Mach numbers and IMF $B_z < 0$ the transpolar potential decreases with increasing B_x. Peng et al. (2010) showed that in the presence of a positive (negative) IMF B_x the merging line shifts northward (southward) on the day side and southward (northward) on the night side. This shift increases with increasing magnitude of IMF B_x. In the Parker spiral the IMF B_x is usually associated with the IMF B_y. It is easy to imagine that in the presence of a finite $B_y < 0$ the dayside reconnection points in both hemispheres would shift northward. It would add the eastward circulation on the dusk side at higher latitudes in the Northern Hemisphere while in the Southern Hemisphere the westward circulation would be added on the dawn side at lower latitudes. In the presence of $B_y > 0$ the westward circulation will be added on the dawn side at lower latitudes in the Northern Hemisphere. In this case a non-zero B_x component may enhance the interhemispheric asymmetry. In particular, in the Northern Hemisphere the effect may result in larger sensitivity of the ESR to the meridional flow on the dawn side.

However, so far we have not found a reasonable explanation of why the nightside maximum is not exactly at midnight but is shifted to ∼03:00 MLT while the paired dayside maximum is exactly at noon. The effect may be caused by unaccounted PCB motion related to localized processes which manifest itself mostly in the (pre-)midnight sector. The post-midnight sector can be the quietest region where the B_y-related azimuthal flow is not suppressed by other kinds of

flow. The temporal PCB motion was demonstrated recently by Laundal et al. (2010). The poleward boundary of the nightside auroral oval under the northward IMF conditions were studied by Lee at al. (2010) using the DMSP data. It was shown that for positive IMF B_y the boundary is more poleward (equatorward) in the premidnight region and the situation is opposite in the postmidnight region and for negative IMF B_y. However, the scattering of the obtained points is rather large. It is worth to check whether the additional asymmetry feature revealed in the present study has been detected by other instruments.

7 Summary

We utilize the unique (more than 1300 h) database collected during 8 yr at the EISCAT Svalbard Radar (around 75 MLat) to infer quantitative characteristics of the east-west ionospheric plasma flow associated with IMF B_y. The following main results were obtained.

1. The effects of IMF B_y are manifested in the intensity and direction of the azimuthal component of the ionospheric flow. The IMF B_y effect is maximal near noon (12:00 MLT) and in the postmidnight (near 03:00 MLT), where its magnitude is about 60 m s^{-1} nT^{-1} for $B_z < 0$ and 40 m s^{-1} nT^{-1} for $B_z > 0$.

2. In the dusk (near 18:00 MLT) and dawn (at 06:00–09:00 MLT) the observed effect is essentially suppressed because of the motion of polar cap boundary associated with the IMF B_y changes.

3. There is indication of a dawn-dusk asymmetry of the magnetosphere. Indeed, for $B_z < 0$, an averaged value of K on the dawn side is twice larger (60 vs. 30 m s^{-1} nT^{-1}), which can not be explained solely by the motion of PCB. The ESR observations presented here provide further evidence for the dawn-dusk asymmetry of the high-latitude magnetosphere-ionosphere coupling.

Acknowledgements. We are indebted to the Director and staff of EISCAT for operating the facility and supplying the data. EISCAT is an international association supported by research organisations in China (CRIRP), Finland (SA), France (CNRS, till end 2006), Germany (DFG), Japan (NIPR and STEL), Norway (NFR), Sweden (VR), and the United Kingdom (STFC). The OMNI data were obtained from CDAWeb. The study was supported by the Academy of Finland projects 115920 (AK) and 132441 (RL).

Topical Editor P.-L. Blelly thanks P. E. Sandholt and another anonymous referee for their help in evaluating this paper.

References

Atkinson, G. and Hutchinson, D.: Effect of the day-night ionospheric conductivity gradient on polar cap convection flow, J. Geophys. Res., 83(A2), 725–729, 1978.

Cowley, S. W. H., Morelli, J. P., and Lockwood, M.: Dependence of convective flows and particle precipitation in the high-latitude dayside ionosphere on the X and Y components of the interplanetary magnetic field, J. Geophys. Res., 96, 5557–5564, 1991.

Hairston, M. R. and Heelis, R. A.: Response time of the polar ionospheric convection pattern to changes in the north-south direction of the IMF, Geophys. Res. Lett., 22(5), 631–634, doi:10.1029/94GL03385, 1995.

Heppner, J. P. and Maynard, N. C.: Empirical high-latitude electric field model, J. Geophys. Res., 92, 4467–4489, 1987.

Jørgensen, T. S., Friis-Christensen, E., and Wilhjelm, J.: Interplanetary magnetic-field direction and high-latitude ionospheric currents, J. Geophys. Res., 77, 1976–1977, 1972.

Kabin, K., Rankin, R., Marchand, R., Gombosi, T. I., Clauer C. R., Ridley, A. J., Papitashvili, V. O., and DeZeeuw, D. L.: Dynamic response of Earth's magnetosphere to B_y reversals, J. Geophys. Res., 108, 1132, doi:10.1029/2002JA009480, 2003.

Khan, H. and Cowley, S. W. H.: Effect of the IMF $B - y$ compon ent on the ionospheric flow overhead at EISCAT: observations and theory, Ann. Geophys., 18, 1503–1522, doi:10.1007/s00585-001-1503-6, 2001.

Kozlovsky, A., Turunen, T., Koustov, A., and Parks, G.: IMF B_y effects in the magnetospheric convection on closed magnetic field lines, Geophys. Res. Lett., 30(24), 2261, doi:10.1029/2003GL018457, 2003.

Laundal, K. M., Ostgaard, N., Snekvik, K., and Frey, H. U.: Interhemispheric observations of emergeing polar cap area, J. Geophys. Res., 115, A07230, doi:10.1029/2009JA015160, 2010.

Lee, D.-Y., Ohtani, S., and Lee, J. H.: On the poleward boundary of the nightside auroral oval under northward interplanetary magnetic field conditions, J. Geophys. Res., 115, A08204, doi:10.1029/2009JA014906, 2010.

Leontyev, S. V. and Lyatsky, W. B.: Electric field and currents connected with Y-component of interplanetary magnetic field, Planet. Space Sci., 22, 811–819, 1974.

Lockwood, M., Sandholt, P. E., Cowley, S. W. H., and Oguti, T.: Interplanetary magnetic field control of dayside auroral activity and the transfer of momentum across the dayside magnetopause, Planet. Space Sci., 37, 1347–1365, 1989.

Lukianova, R. and Christiansen, F.: Modeling of the global distribution of ionospheric electric fields based on realistic maps of field-aligned currents, J. Geophys. Res., 111, A03213, doi:10.1029/2005JA011465, 2006.

Lukianova, R., Kozlovsky, A. and Turunen, T.: Comparison and validation studies related to the modeling ionospheric convection and the European incoherent scatter observations in the polar cap, Int. J. Geomagn. Aeron., 7(3), GI3005, doi:10.1029/2007GI000169, 2008.

Lyatsky, W. B.: Current systems of the magnetosphere-ionosphere disturbances, Nauka, St. Petersburg, Russia, 192 pp., 1978 (in Russian).

Lyons, L. R., Liu, S., Ruohoniemi, J. M., Solovyev, S. I., and Samson, J. C.: Observations of Dayside Convection Reduction Leading to Substorm Onset, J. Geophys. Res., 108(A3), 1119, doi:10.1029/2002JA009670, 2003.

Nishida, A.: Interplanetary origin of electric fields in the magnetosphere, Cosmic Electrodyn., 2, 350–374, 1971.

Papitashvili, V. O. and Rich, F. J.: High-latitude ionospheric convection models derived from Defense Meteorological satellite Program ion drift observations and parameterized by the interplanetary magnetic field strength and direction, J. Geophys. Res., 107(A8), 1198, doi:10.1029/2001JA000264, 2002.

Park, K. S., Ogino, T., and Walker, R. J.: On the importance of antiparallel reconnection when the dipole tilt and IMF By are nonzero, J. Geophys. Res., 111, A05202, doi:10.1029/2004JA010972, 2006.

Peng, Z., Wang, C., and Hu, Y. Q.: Role of IMF B_x in the solar wind-magnetosphere-ionosphere coupling, J. Geophys. Res., 115, A08224, doi:10.1029/2010JA015454, 2010.

Ridley, A. J., Lu, G., Clauer, C. R., and Papitashvili, V. O.: A statistical study of the ionospheric convection response to changing interplanetary magnetic field conditions using the assimilative mapping of ionospheric electrodynamics technique, J. Geophys. Res., 103(A3), 4023–4039, doi:10.1029/97JA03328, 1998.

Ruohoniemi, J. M. and Greenwald, R. A.: Dependencies of high-latitude plasma convection: Consideration of IMF, seasonal, and UT factors in statistical patterns, J. Geophys. Res., 110, A09204, doi:10.1029/2004JA010815, 2005.

Sandholt, P. E. and Farrugia, C. J.: Poleward moving auroral forms (PMAFs) revisited: responses of aurorae, plasma convection and Birkeland currents in the pre- and postnoon sectors under positive and negative IMF B_y conditions, Ann. Geophys., 25, 1629–1652, doi:10.5194/angeo-25-1629-2007, 2007.

Sandholt, P. E. and Farrugia, C. J.: Plasma flow channels at the dawn/dusk polar cap boundaries: momentum transfer on old open field lines and the roles of IMF B_y and conductivity gradients, Ann. Geophys., 27, 1527–1554, doi:10.5194/angeo-27-1527-2009, 2009.

Stern, D. P.: A study of the electric field in an open magnetospheric model, J. Geophys. Res., 78, 7292–7305, 1973.

Svalgaard, L.: Polar cap magnetic variations and their relationship with the interplanetary magnetic sector structure, J. Geophys. Res., 78, 2064–2078, 1973.

Trondsen, T. S., Lyatsky, W., Cogger, L. L., and Murphree, J. S.: Interplanetary magnetic field B_y control of dayside auroras, J. Atmos. Sol.-Terr. Phy., 61, 829–840, 1999.

Tsyganenko, N. A. and Sitnov, M. I.: Modeling the dynamics of the inner magnetosphere during strong geomagnetic storms, J. Geophys. Res., 110, A03208, doi:10.1029/2004JA010798, 2005.

Watanabe, M., Sofko, G. J., Kabin, K., Rankin, R., Ridley, A. J., Clauer, C. R., and Gombosi, T. I.: Origin of the inter-hemispheric potential mismatch of merging cells for interplanetary magnetic field B_y-dominated periods, J. Geophys. Res., 112, A10205, doi:10.1029/2006JA012179, 2007.

Zhang, S.-R., Holt, J. M., and McCready, M.: High latitude convection based on long-term incoherent scatter radar observations in North America, J. Atmos. Sol.-Terr. Phy., 69, 1273–1291, 2007.